THE ANECHOIC FLOW FACILITY - AERODYNAMIC CALIBRATION AND EVALUATION

Brian E. Bowers

Naval Ship Research and Development Center
Bethesda, Maryland

May 1973

THE ANECHOIC FLOW FACILITY - AERODYNAMIC CALIBRATION AND EVALUATION

SAD-48E-1942

NAVAL SHIP RESEARCH AND DEVELOPMENT CENTER
Bethesda, Maryland 20034

THE ANECHOIC FLOW FACILITY - AERODYNAMIC CALIBRATION AND EVALUATION

by

Brian E. Bowers

SHIP ACOUSTICS DEPARTMENT

EVALUATION REPORT

May 1973

SAD-48E-1942

The Naval Ship Research and Development Center is a U. S. Navy center for laboratory effort directed at achieving improved sea and air vehicles. It was formed in March 1967 by merging the David Taylor Model Basin at Carderock, Maryland with the Marine Engineering Laboratory at Annapolis, Maryland.

Naval Ship Research and Development Center
Bethesda, Md. 20034

MAJOR NSRDC ORGANIZATIONAL COMPONENTS

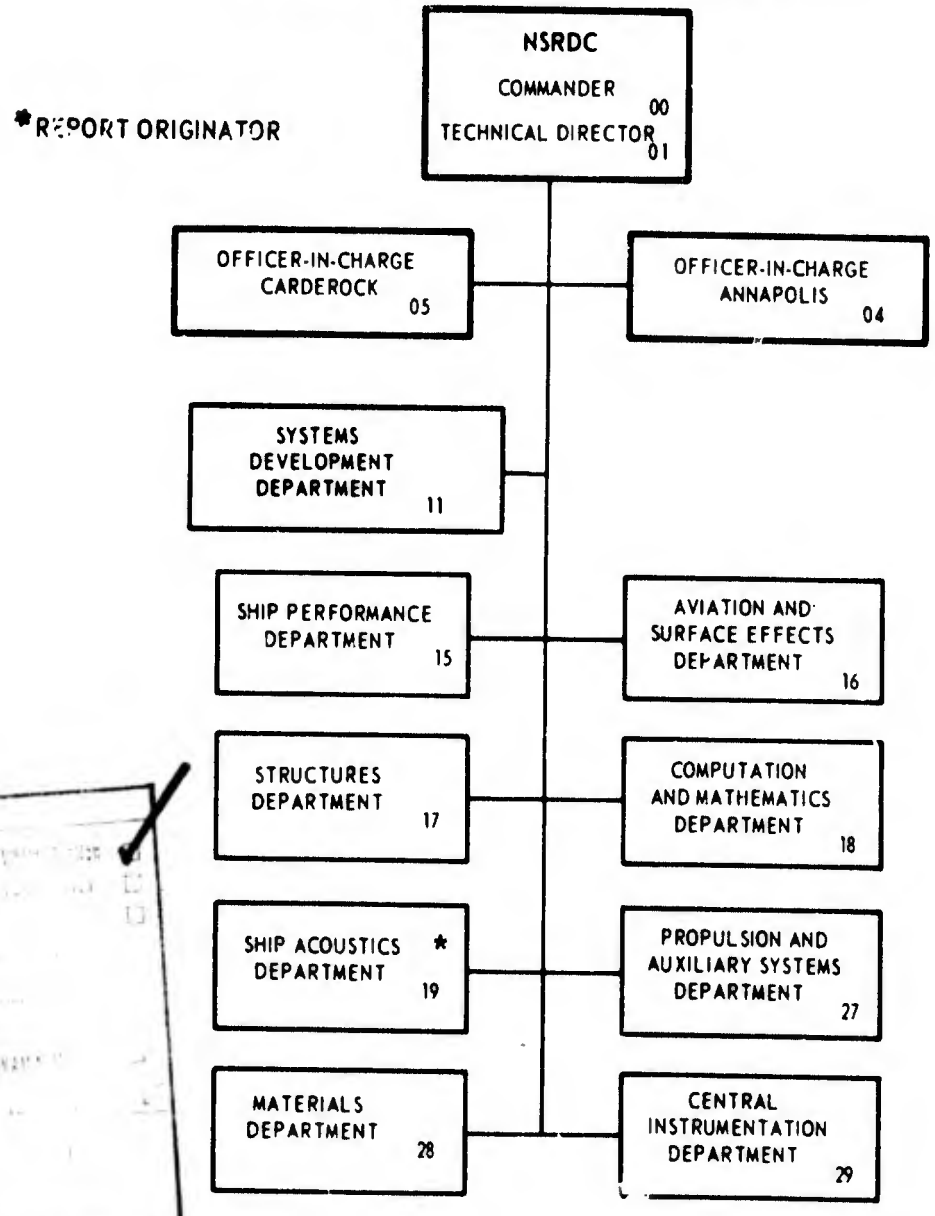

*REPORT ORIGINATOR

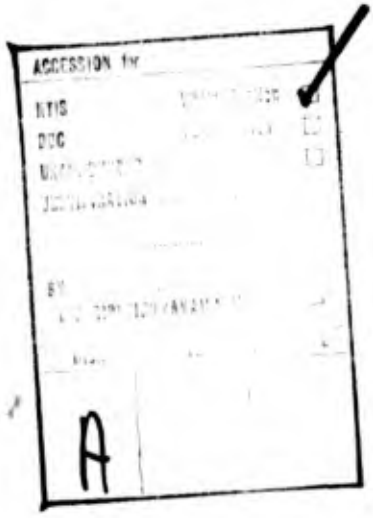

UNCLASSIFIED
Security Classification

DOCUMENT CONTROL DATA - R & D

Security classification of title, body of abstract and indexing annotation must be entered when the overall report is classified)

1. ORIGINATING ACTIVITY (Corporate author)
Naval Ship Research and Development Center
Bethesda, Maryland 20034

2a. REPORT SECURITY CLASSIFICATION
UNCLASSIFIED

2b. GROUP

3. REPORT TITLE
THE ANECHOIC FLOW FACILITY - AERODYNAMIC CALIBRATION AND EVALUATION

4. DESCRIPTIVE NOTES (Type of report and inclusive dates)
Evaluation report

5. AUTHOR(S) (First name, middle initial, last name)
Brian E. Bowers

6. REPORT DATE	7a. TOTAL NO. OF PAGES	7b. NO. OF REFS
May 1973	~~44~~ 45	5

8a. CONTRACT OR GRANT NO	9a. ORIGINATOR'S REPORT NUMBER(S)
b. PROJECT NO 1-1942-034-01	SAD-48E-1942
c.	9b. OTHER REPORT NO(S) (Any other numbers that may be assigned this report)
d.	

10. DISTRIBUTION STATEMENT
Approved for Public Release: Distribution Unlimited

11. SUPPLEMENTARY NOTES	12. SPONSORING MILITARY ACTIVITY
Details of illustrations in this document may be better studied on microfiche	Naval Ship Systems Command, Code 037

13. ABSTRACT

Since 14 May 1971, the new Anechoic Flow Facility at the Naval Ship Research and Development Center has been undergoing periodic operational exercises and calibrations to determine the extent to which the facility may be used in the study of flow-induced noise. Some preliminary results are available with respect to both acoustical and aerodynamic calibrations although both have yet to be completed due to other higher priority programs which must be phased into the facility test schedule. Purpose of this report is to evaluate the aerodynamic performance characteristics of the Anechoic Flow Facility with regard to the established design specifications and to present some preliminary aerodynamic calibration data.

DD FORM 1 NOV 68 1473 (PAGE 1)
S/N 0101-807-6801

UNCLASSIFIED
Security Classification

14 KEY WORDS	LINK A		LINK B		LINK C	
	ROLE	WT	ROLE	WT	ROLE	WT
Anechoic						
Calibration						
Aerodynamic						
Evaluation						

TABLE OF CONTENTS

LIST OF FIGURES

LIST OF FIGURES (Cont)

LIST OF TABLES

LIST OF SYMBOLS

b	Barometric Pressure, inches Hg
e_w	Saturated Vapor Pressure, inches Hg
h	Relative Humidity, (Dry=0, Saturated = 1.0)
K	Calibration Coefficient
P_d	Dynamic Pressure
P_s	Static Pressure
P_t	Total Pressure
S	Relative Density of Water Vapor, lbmass/lbmass
S.G.	Specific Gravity, (Air, S.G. = 1.0)
T	Temperature, ^oF
TI	Percent Turbulence Intensity
U_∞, V	Free-stream Velocity or Tunnel Speed
u	Longitudinal Component of Velocity
v	Transverse Component of Velocity Normal to Walls
w	Transverse Component of Velocity Normal to Floor and Ceiling
y	Direction Normal to Test Section Walls
δ	Boundary Layer Thickness
ρ	Density of air, $lbmass/ft^3$
μ	Absolute Viscosity, $\frac{lbforce\text{-}sec}{ft^2}$
ν	Kinematic Viscosity, $\frac{ft^2}{sec}$
DP	Dew Point Values
DB	Dry Bulb values
TS	Test Section Values

ABSTRACT

Since 14 May 1971, the new Anechoic Flow Facility at the Naval Ship Research and Development Center has been undergoing periodic operational exercises and calibrations to determine the extent to which the facility may be used in the study of flow-induced noise. Some preliminary results are available with respect to both acoustical and aerodynamic calibrations although both have yet to be completed due to other higher priority programs which must be phased into the facility test schedule. To date, the aerodynamic performance characteristics of the Anechoic Flow Facility meet in all respects the established design specifications. Some preliminary aerodynamic calibration data is presented.

INFORMATION INFORMATION

The work reported herein was funded by the Naval Ship Systems Command under subproject SF 43 452 007, Task 10442.

INTRODUCTION

The Naval Ship Research and Development Center (NSRDC) Anechoic Flow Facility (AFF) is a low-turbulence closed-loop wind tunnel with an anechoic chamber. The chamber surrounds an open-jet section allowing an essentially free-field environment in which to measure flow-induced noise. Proper utilization of acoustical materials minimizes the operational noise of the tunnel itself.[1]

To properly calibrate a facility of this type, both aerodynamic and acoustical measurements must be made, often identifying a particular flow

[1] A complete listing of references is given on page 37.

pattern or phenomenon with the noise it generates. The preliminary aerodynamic calibrations and investigations to be covered by this Evaluation Report are those made in the closed-jet test section. Further aerodynamic calibrations will be performed in the anechoic chamber (open-jet test section) as the test schedule permits.

AFF PHYSICAL CHARACTERISTICS

A brief description of the physical characteristics will now be presented emphasizing the open- and closed-jet test sections. Figures (1) and (2) depict the physical characteristics and dimensions of the tunnel circuit. Figure (3) is an enlarged drawing of the essential part of the north leg of the AFF. The facility can be considered to have two test sections, the closed-jet test section (essentially a constant area duct) and the open-jet test section (turbulent free jet in the anechoic chamber). The "constant area duct" is actually not constant area, but has an area expansion rate of 0.031 $ft.^2$ per ft. to account for the growth of the boundary-layer displacement thickness and hence to maintain a zero pressure gradient along this section.

Two piezometer rings of 12 static pressure taps each (three to a side) are located in the walls of the contraction section and are 40.5 and 14 feet from the nozzle lip. The 12 taps are connected by a manifold thus giving an average static pressure for that cross-section. Individual static pressure taps are also located in the ceiling and walls at 8.83 and 7.83 feet from the nozzle exit respectively.

The collector cowl could be considered the most difficult element to design in a facility of this type. It must possess acoustical

characteristics to absorb incident sound, and yet be aerodynamically efficient to collect the flow while maintaining a fixed stagnation point. Furthermore, it must be structurally rigid to resist the aerodynamic loading so as to minimize the noise due to the flow. A diffuser section is located immediately downstream of the collector cowl. Figures (4) through (9) are photographs showing these essential features of the AFF. Figure (4) was taken in the anechoic chamber looking upstream into the 8 foot closed-jet test section. The final anti-turbulence screen can be seen upstream. Static pressure plates, the cover plate of the instrument trench, and the observation window are also visible. Figure (5) was taken in the collector cowl looking upstream through the closed-jet test section toward the anti-turbulence screens. Notice the aerodynamic model support in the closed-jet test section and the wire floor in the anechoic chamber. Figures (6) and (7) were taken in the anechoic room showing the nozzle and collector cowl respectively. The downstream diffuser and turning vanes are also shown in Figure (7). Figures (8) and (9) show different views of the anti-turbulence screens and contraction section.

Pertinent facility parameters are listed in Appendix A.

VELOCITY PERFORMANCE CALIBRATION

A calibrated pitot-static tube was mounted in the closed-jet test section and its output was monitored along with both upstream piezometer rings over the entire speed range of the tunnel. By relating the dynamic pressure output of the pitot-static tube to the corresponding upstream differential static pressure output, ΔP_s, of the piezometer rings, one will

be able to utilize these dynamic pressures (without pitot-static tube) in later tests and experiments simply by knowing what these differential static pressures are and using them as indicators of the flow velocity. The output of a pitot-static tube is the total pressure (orifice normal to flow direction). These pressure outputs were connected to the AFF 50-tube, 100 inch manometer board. Since

$$P_d = P_t - P_s = 1/2\ \rho U_\infty^2, \tag{1}$$

where, P_d is the dynamic pressure;

P_t is the total pressure;

P_s is the static pressure;

ρ is the air density;

U_∞ is the flow velocity,

one may determine the flow velocity by reading the difference between P_t and P_s on the manometer. The density of the air is calculated from measurements of dry-bulb and dew-point temperatures, barometric pressure, and test-section static pressure. Taking into account the calibration coefficient of the pitot-static tube, the equation above is used in the following form to calculate the velocity:

$$U_\infty = 16.363\ \left(\frac{K\ P_d}{\rho}\right)^{1/2}, \tag{2}$$

where, K is the calibration coefficient of pitot-static tube;

U_∞ is in units of ft/sec;

P_d is in units of inches alcohol;

ρ is in units of lbm/ft^3.

The equation used for the calculation of density is presented in Appendix B.

Once a velocity calibration of the unique relationship between ΔP_s and U is established, it is a simple matter to dial in a particular tunnel velocity. First, the ΔP_s corresponding to the desired velocity is dialed into the micromanometer on the console and next, the RPM of the fan drive system is slowly adjusted until the micromanometer gauge nulls, indicating that the intended velocity has been attained.

Figure (10) is a velocity calibration curve for a clean tunnel condition, i.e., no models or fixtures mounted in either test section. Also plotted on Figure (10) is the data obtained with two different NSRDC model bodies-of-revolution mounted in the closed-jet test section. This figure therefore shows the typical solid blockage-interference effect involving increased axial velocity due to the partial blockage of the flow in the closed jet. The blockage effect becomes more important at high tunnel speeds and would necessitate a new velocity calibration with the model in place in the tunnel, especially for the planned larger twenty-foot models.

The low-speed velocity calibration was performed by a Davis Instrument Co. vane-type anemometer and the results are plotted in Figure (11).

Other operational performance information of secondary importance such as the fan RPM and test section static pressure variation with tunnel velocity is presented in Figures (18) and (19). The calibration of the Aerolab velocity gauge is shown in Figure (20). Indications of facility warm-up time and tunnel speed-temperature stability is presented in Figures (21) and (22).

CROSS-SECTIONAL VELOCITY DISTRIBTUION

As in any wind tunnel, non-uniformities in the mean velocity exist in planes normal to the flow direction. Since parallel flow of uniform velocity is desirable, dynamic pressure measurements at chosen cross-sections in the closed-jet test section were carried out to determine the velocity distribution. For this purpose, the Aviation and Surface Effects Department 8-foot survey rake was used in conjunction with the AFF 100-inch, 50-tube manometer. The survey rake had 14 pitot-static tubes mounted at 6 inch intervals. Aluminum brackets were utilized so that the rake could be moved laterally both in the vertical and horizontal positions allowing calculations of velocity to be made in a 6-inch mesh pattern. Figures (12) and (13) are photographs showing typical survey rake installations.

The cross-sectional velocity distribution was measured for several axial positions in the closed-jet test section. Figure (14) is a typical cross-sectional velocity distribution measured in a plane 53 3/16 inches from the nozzle lip. The data is presented as percentage deviations from the mean velocity of 203.1 ft/sec. The experimental error in obtaining this data is 0.5% of the mean velocity.

MEASUREMENTS OF FREE-STREAM TURBULENCE INTENSITY

In a typical wind tunnel, the air stream is never completely uniform and steady. In particular, small eddies of varying size and intensity are always present and are referred to collectively as the turbulence of the stream. It is important to differentiate between the time-variations of velocity which constitute the turbulence (the mean over a sufficiently long time period being zero) and the large-scale spatial variations which are usually referred to as non-uniformity or by some similar term.

In order that the results of wind-tunnel measurements may be applied to the conditions of free unbounded flow without serious error, one of the principal objectives of a wind tunnel design is to minimize the intensity of the free-stream turbulence of the flow in the working section. The free-stream turbulence intensity design specification of the AFF was stipulated to be 0.1% or less and measurements were made to corroborate this specification.

A measure of the strength of the disturbances in the free-stream can be found by determining the time average of the fluctuating, turbulent velocities u'^2, v'^2, w'^2. Since the turbulence intensity or level is defined as

$$TI = \frac{\sqrt{1/3(\overline{u'^2} + \overline{v'^2} + \overline{w'^2})}}{U_\infty}, \tag{3}$$

TI can be calculated. If measurements of the fluctuating velocities are made sufficiently far downstream from the screens so that the reduced large scale vortices decay sufficiently, then the mean oscillations approach equivalent values, and the flow becomes isotropic or

$$u'^2 = v'^2 = w'^2, \tag{4}$$

which reduces equation (3) to

$$TI = \frac{\sqrt{\overline{u'^2}}}{U_\infty}. \tag{5}$$

During the initial attempts to measure the clean tunnel free-stream turbulence intensity with a Flow Corporation Model 900 constant temperature hot-wire anemometer system, it was readily apparent that the electronic and vibrational noise levels of the measuring system had at least the same magnitude as the turbulence existing in the tunnel. Since turbulence intensities in the neighborhood of 0.14% were being measured, it was felt at the time that this was actually system noise and that the free-stream turbulence intensity was decidedly lower.

In a further attempt to determine the AFF free-stream turbulence intensity in the closed jet, R. Dwyer and W. Blake used a Disa Model 55D05 battery powered constant temperature system with a probe on the longitudinal centerline 2 feet from the nozzle lip and measured percentage values of 0.12. Again, after these measurements were taken, it was felt that the signal level was lower than the electronic noise and that the turbulence intensity was actually on the order of 0.1%.

F. DeMetz and R. Stern again used the Flow Corporation Model 900E constant temperature system in a very carefully planned procedure utilizing proper filtering and measured turbulence intensities which were less than the specification of 0.1%. DeMetz, et al., further repeated these measurements with a Flow Corporation Model HWB-3 battery powered constant current system while another test was being carried on. The resulting values, however, were obtained only 13 inches from a wall.

Later, with a clean tunnel condition, DeMetz and J. Helmandollar made measurements on the tunnel axis and also across the closed-jet test section for various velocities and again obtained turbulence intensity values of around 0.1%.

The above measurements are presented in concise detail in Table (1). The heading "Tunnel Condition" indicates whether models or fixtures were present during the turbulence intensity measurement or if the tunnel was in a clean condition. It must be kept in mind that some of these measurements may not be indicative of the actual turbulence intensity of the free-stream but represent electronic and mounting noise of the instrumentation.

BOUNDARY LAYER ON WALLS

Most tests carried out in wind tunnels require that a model be located entirely in uniform parallel flow and away from the flow influenced by the wall boundary. Therefore, it is necessary to survey the wall boundary layer within the closed-jet test section. An overall estimate of this boundary-layer thickness can be determined from the cross-sectional velocity calibration data as shown in Figure (14). All of these data seem to indicate that in the nozzle area of the closed-jet test section the wall boundary layer is of the order of one foot thick. This is taken as a general condition however, and should only be used as a rule of thumb.

Specific regions, however, require more careful measurements. For example, the north wall (between the tunnel door and the nozzle) has two probe-access holes where various probes may be easily inserted to measure the flow properties. For this purpose, a pitot-static tube was mounted at the upstream probe-access hole to measure the boundary-layer thickness as the tunnel was run at various velocities. Figure (15) shows a plot of these measurements. The theoretical prediction shown is that for a flat plate, zero pressure gradient boundary-layer growth. Since the tunnel is a closed circuit, a value of x (distance from leading edge) was calculated by

using one of the measured data points and then assumed to be a virtual leading edge for the other calculations.

F. DeMetz, in carrying out his work on a flat-plate prototype model mounted vertically to the floor, made measurements of the boundary layer on the floor at a distance of 5.38 inches from the plate surface, well out of the plate boundary layer. His measurements were made 195.75 inches upstream of the nozzle lip and a distance of 73.75 inches upstream of the previously mentioned wall boundary-layer measurements taken at the probe access hole. Figures (16) and (17) show the resultant velocity profiles. For the two velocities considered, DeMetz determined the boundary layer to be 2 inches thick. Assuming flat-plate boundary-layer growth with zero pressure gradient, the boundary layer on the floor would be 3.1 inches adjacent to the wall probe access hole. Hence both measurements agree quite well especially since a slight negative pressure gradient does exist which tends to reduce boundary-layer growth.

TUNNEL WALL FLOW SEPARATION

Turbulent boundary-layer separation on tunnel walls causes energy to be lost and hence the efficiency of the powering unit to drop. Ordinarily, this occurs in the downstream diffuser section where separation results in surging or low-frequency velocity pulsations which may cause problems in maintaining steady conditions when measurements are made.

In the AFF, wall boundary-layer separation is most critical in the wide-angle diffuser just upstream of the anti-turbulence screens and in the diffuser section downstream of the anechoic chamber. These two tunnel

sections both possess the one factor which can cause wall separation, i.e., an increasing or positive pressure gradient. The design of the wide-angle diffuser was based on research carried out by Schubauer and Spangenberg[2], which shows that the proper utilization of screens with a wide-angle diffuser tends to prevent separation by specifying periodic pressure drops (screens) during the rapid increase in pressure gradient in the diffuser. The AFF wide-angle diffuser has a maximum included angle of 60 degrees occurring over a span of 12.21 feet. As can be seen from Figure (2), the inside turning angle for the flow is 290 degrees which is quite a large value. One-eighth scale model tests of the AFF conducted in February 1964 by Northern Research and Engineering Corporation[3] indicated that separation did occur on this inside corner.

The downstream diffuser, however, has an included angle of approximately 5 degrees. For diffusers of this type the maximum allowable included angle is 6 degrees.

To determine whether separation occurs in these two tunnel sections, tufts were placed on a long pole and moved vertically and horizontally along the walls and floor for various fan speeds so that regions of reversed flow could be detected. No flow reversal was found in the wide-angle diffuser for fan speeds of 0-370 RPMs, and in the downstream diffuser for fan speeds up to 170 RPMs (could no higher due to high velocities encountered).

Normally, wall separation would not be too critical in a wind tunnel since its most serious effects would be to interfere with balance measurements. In the case of the anechoic low-turbulence facility, however, the presence of separation might interfere greatly with hot-wire and acoustical measurements. This is mentioned because there exists other regions of

adverse pressure gradient which are less critical than the areas already mentioned yet at some future time may cause difficulties for some particular experiments.

CONCLUSIONS

The aerodynamic design specifications of the Anechoic Flow Facility have been met with complete satisfaction. Further tests and evaluation, however, will be carried out on the AFF to determine those characteristics not covered in the design specifications.

RECOMMENDATIONS FOR FUTURE EVALUATIONS

It is always good practice to perform additional velocity calibrations when the conditions surrounding a particular test deviates substantially from those which normally exist. Velocity calibrations should also be made or confirmed prior to an experiment if the investigator desires an accuracy of less than $\pm 1\%$. Day to day changes in the air density are usually insignificant but weekly or monthly changes could result in errors of 2 percent or more until several seasonal velocity calibrations are performed. These velocity calibrations should be made with the planned test models or fixtures mounted in the tunnel because of the associated blockage effect on tunnel speed.

Periodic checks, however, will be made to verify the velocity calibrations, free-stream turbulence intensity, test-section cross-sectional velocity profile, and test-section flow non-uniformities for the clean tunnel condition.

Planned future evaluation of the flow characteristics of the AFF closed- and open-jet test sections are listed as follows:

CLOSED-JET TEST SECTION

1. Further evaluate the free-stream turbulence intensity
2. Determine the extent of isotropy of turbulence
3. Determine the direction of flow or degree of swirl at several cross-sections.

OPEN-JET TEST SECTION

1. Determine cross-sectional velocity profile of turbulent free jet for several tunnel speeds.
2. Determine width of shear layer of turbulent free jet as a function of flow direction.
3. Investigate the divergence of the turbulent free jet across the anechoic chamber.
4. Determine the magnitude, direction, and dimensions of the secondary flow pattern in the anechoic chamber.

ACKNOWLEDGMENTS

Many individuals of the Naval Ship Research and Development Center staff were involved in making the AFF operational and providing technical assistance in establishing calibration and evaluation exercises for the facility. In particular, Messrs. Joseph O'Donnell, R. William Brown, Thomas C. Mathews, and James A. Padgett of the Ship Acoustics Department were instrumental in making the AFF operational, in establishing and in executing the calibration and evaluating procedures.

Special acknowledgment is given to John Kohlhafer and Eugene Curtis of the Industrial Department for their valuable efforts in obtaining the aerodynamic data, and to Ted Farabee, Rich Stern, and William Hoover of Ship Acoustics Department for their help in reducing some of the data.

Special acknowledgment is also given to Dr. Fred C. DeMetz of Ship Acoustics Department for his assistance in obtaining most of the turbulence intensity measurements.

APPENDIX A

PERTINENT FACILITY CHARACTERISTICS

Number of screens	8
Mesh size	14 to the inch
Diameter of wire	0.021 inches
Solidity ratio	0.5
Contraction ratio (area)	10:1
Diameter of closed-jet test section	8 foot octagonal
Length of closed-jet test section	8 feet-11 inches
Dimensions of Anechoic room	17'-1" X 19'-6" X 19'-6" (LHW)
Cut-off frequency of acoustic wedges	140 Hz
Average rms roughness of concrete walls	400 μ inches rms
Maximum model length	20 feet
Usable open volume area of anechoic chamber	1698 ft^3
Maximum allowable velocity	200 ft/sec
Minimum controllable velocity	14 ft/sec
Turbulence intensity in free-stream	$\leq$ 0.1%
Fan designed flow rate	7×10^5 cfm @500 rpm, ΔP = 12 in H_2O

APPENDIX B

CALCULATION OF AIR DENSITY

Using the Perfect Gas Equation of State and the Gibbs-Dalton rule concerning partial pressure, an expression[4] for the density of a gas can be written as

$$\rho = \frac{(b-e_w h)(S.G.) + e_w hs}{346.5 + 0.7535\ T} \qquad \text{(B-1)}$$

where b is barometric pressure (inches Hg)

T is dry-bulb temperature (^{o}F)

h is relative humidity (dry = 0, sat = 1.0)

S.G. is specific gravity

e_w is saturated vapor pressure (inches Hg)

ρ is gas density (lbm/ft^3)

and $s = 0.6214 + \frac{h(e_w)^{0.704}}{1130}$ is the relative density ($\frac{lb}{lb}$). For air, S.G. = 1.0, therefore Equation (B-1) becomes

$$\rho = \frac{b - e_w h(1-S)}{346.5 + 0.7535\ T} \qquad \text{(B-2)}$$

Applying Equation (B-2) to our particular case, one must make the following adjustments. The barometric pressure, b, is the pressure exerted on a particle of air. Since a very slight negative static pressure exists in the test section for essentially the whole speed range, the pressure, exerted on a particle of air in the test section is the barometric pressure, b, as measured in the control room minus the test section static pressure, $(P_s)_{T.S.}$, as measured by the three static pressure plates in the test section. Therefore, Equation (B-2) becomes

$$\rho = \frac{[b - (P_s)_{TS}] - e_w h(1-S)}{346.5 + 0.7535\ T} \qquad (P-3)$$

Values of b, $(P_s)_{T.S.}$, T are recorded from gauges located in the control room. Values of e_w and h can be found from published tables once T and $T_{D.P.}$ (dew point temperature) are known. S is calculated from the previously presented relationship.

Combining Equations (2) and (B-3), the flow velocity then becomes

$$U_\infty = 16.363 \left[\frac{K\ P_d(346.5 + 0.7535\ T)}{[b-(P_s)_{TS}] - e_w h\ [1-(0.6214 + h(e_w)^{.704})]} \right]^{1/2} \qquad (B-4)$$

Thus for any dynamic pressure sensed by a pitot-static tube of calibration coefficient K, the tunnel speed can be calculated by recording and using the corresponding values of T, b, $(P_s)_{T.S.}$, and $T_{D.P.}$.

Once the tunnel is velocity calibrated for a particular test, day to day changes in ρ would result in only small errors in velocity. The magnitude of these errors has been calculated and has never been found to be greater than $\pm 1\%$ of the maximum velocity.

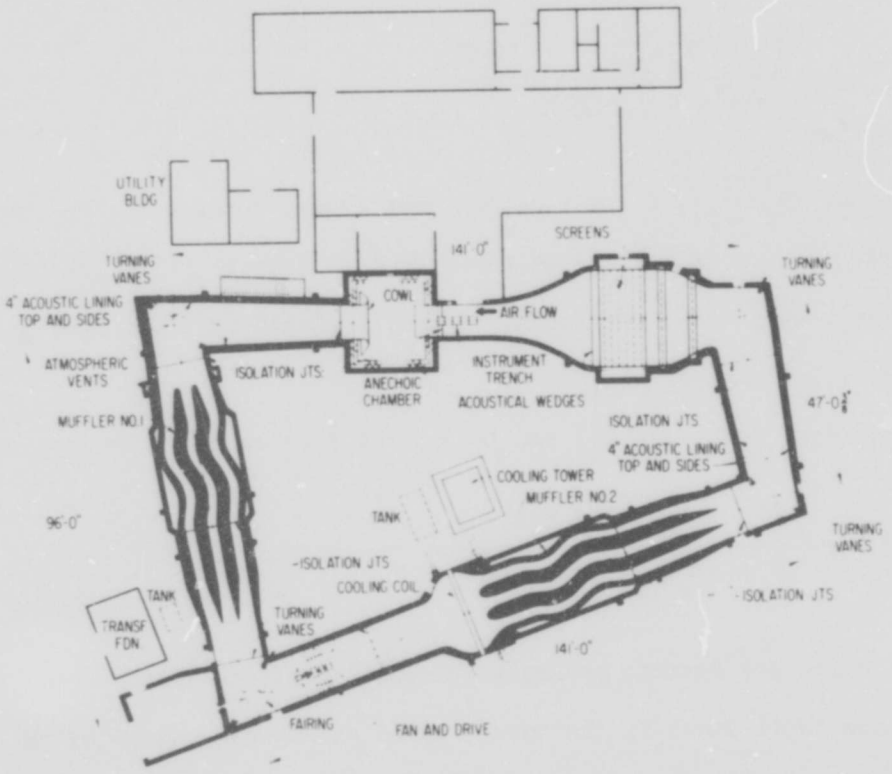

Figure 1 - Plan View of Physical Characteristics of NSRDC Anechoic Flow Facility

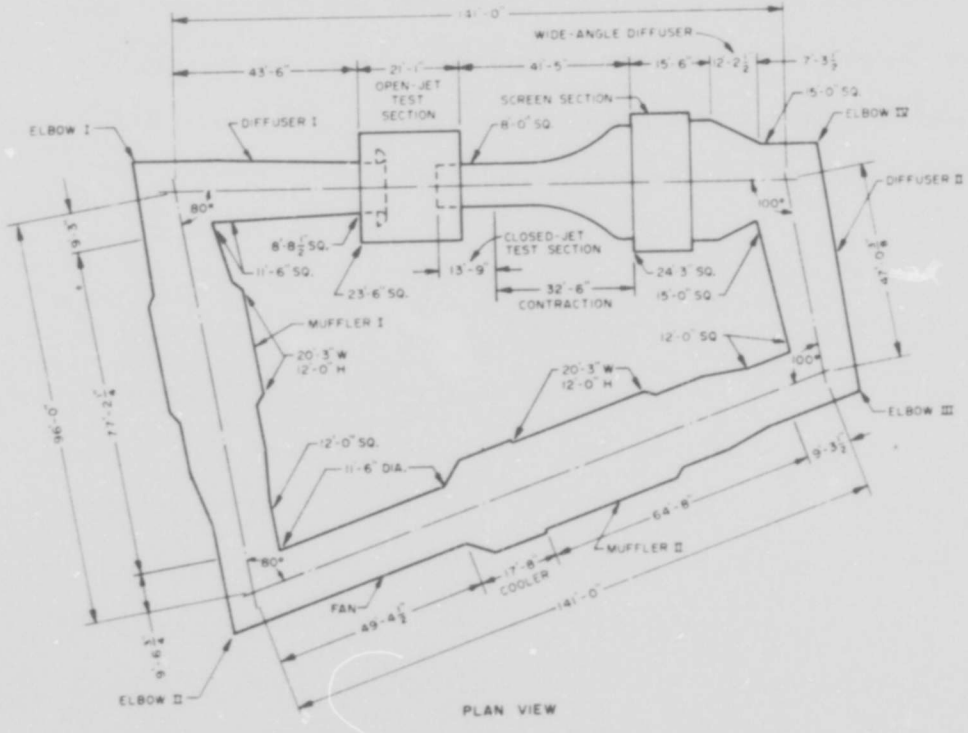

Figure 2 - Physical Dimensions of the AFF Tunnel Circuit

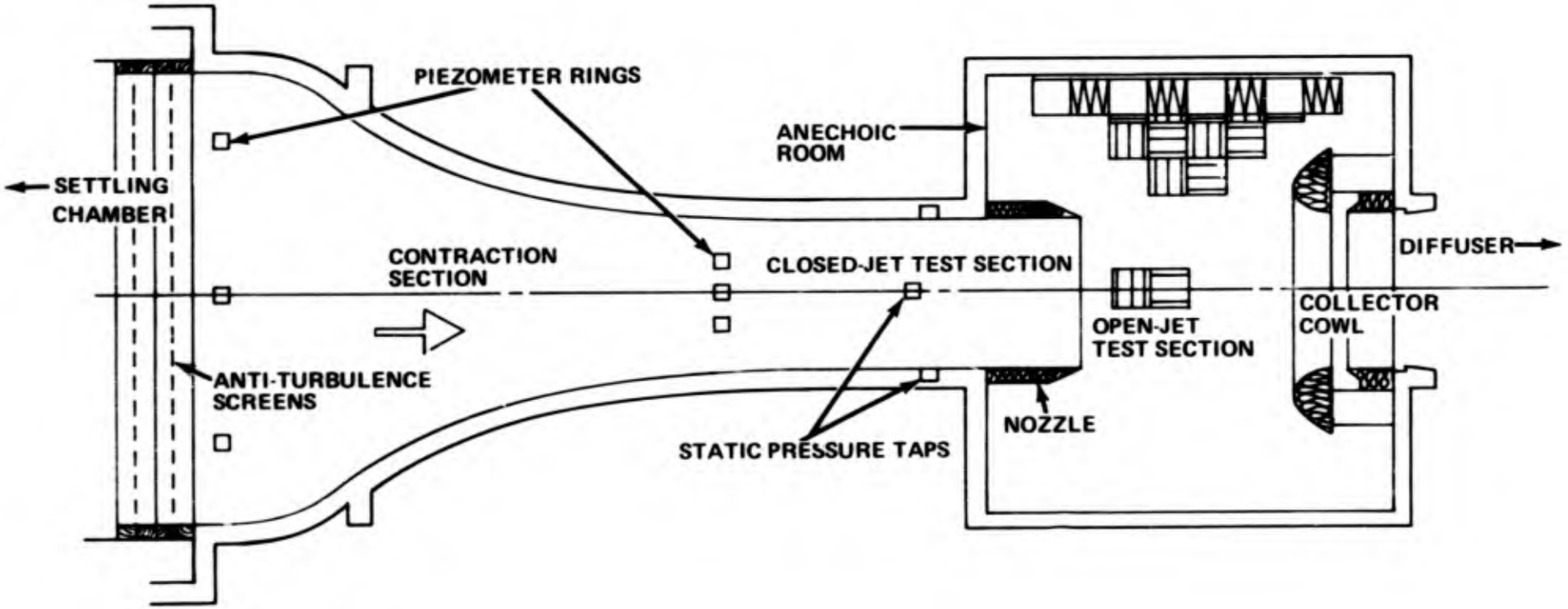

Figure 3 - Cutaway Plan View of Test Sections and Anechoic Room

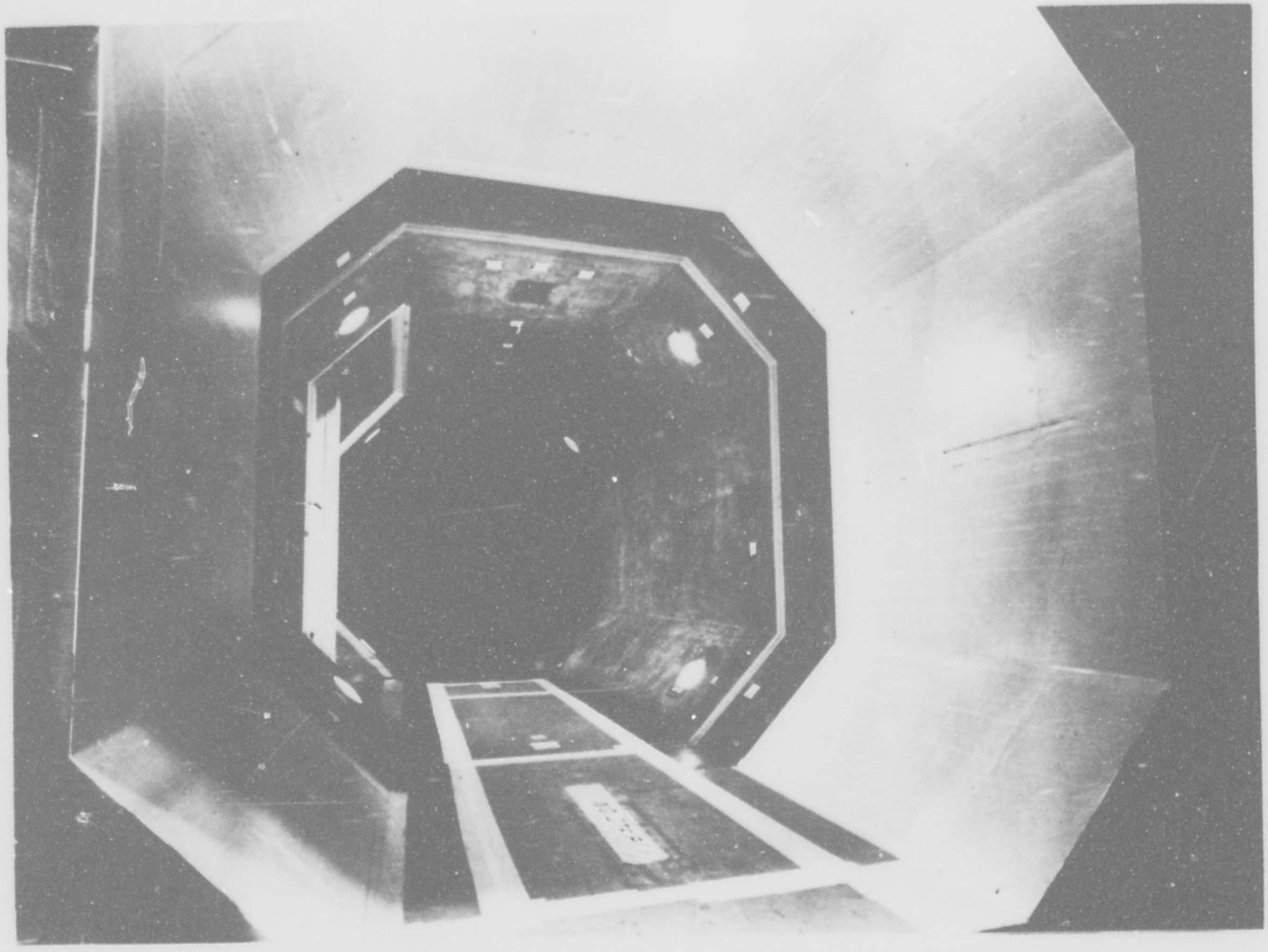

Figure 4 - View of Closed-Jet Test Section Looking Upstream from Anechoic Chamber.

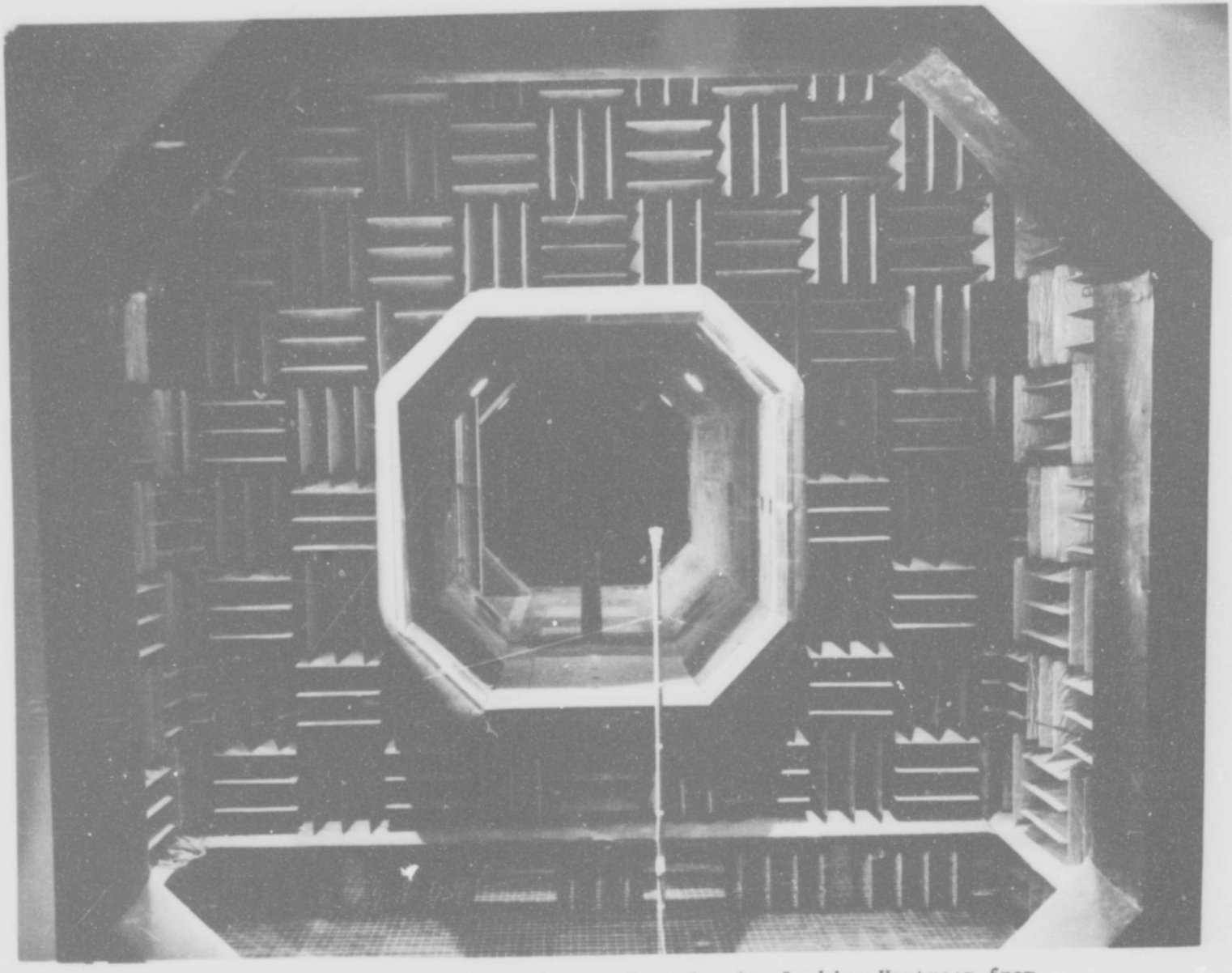

Figure 5 - View of Open- and Closed-Jet Test Section Looking Upstream from Collector Cowl

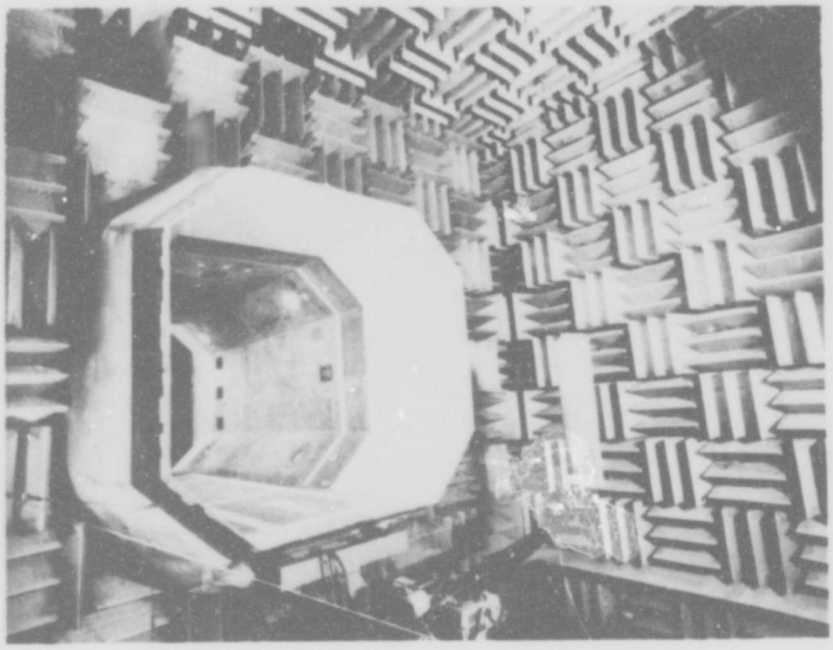

Figure 6 - Photograph of Open-Jet Nozzle as seen from Anechoic Chamber

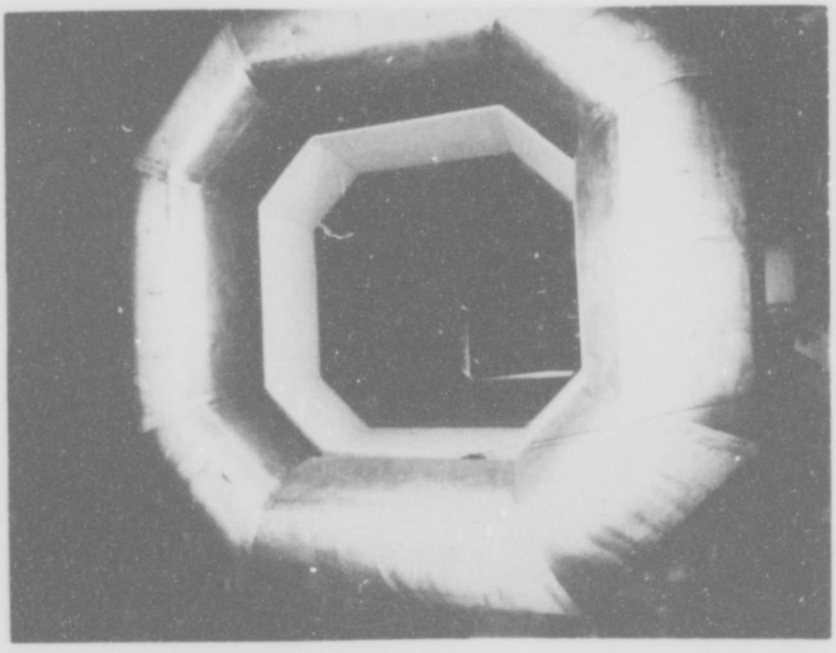

Figure 7 - Photograph of Collector Cowl as seen from Anechoic Chamber

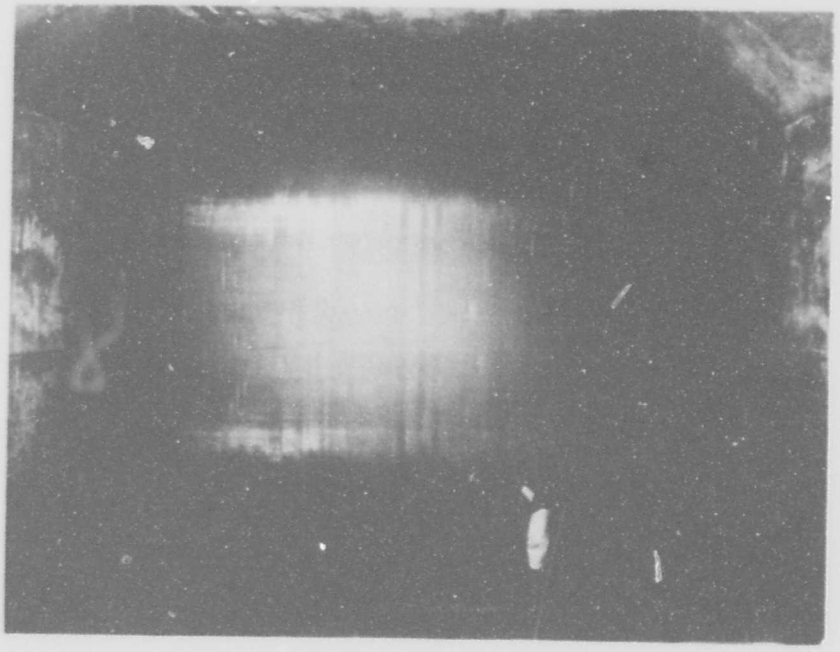

Figure 8 - Upstream View of Final Anti-Turbulence Screen and Contraction Section

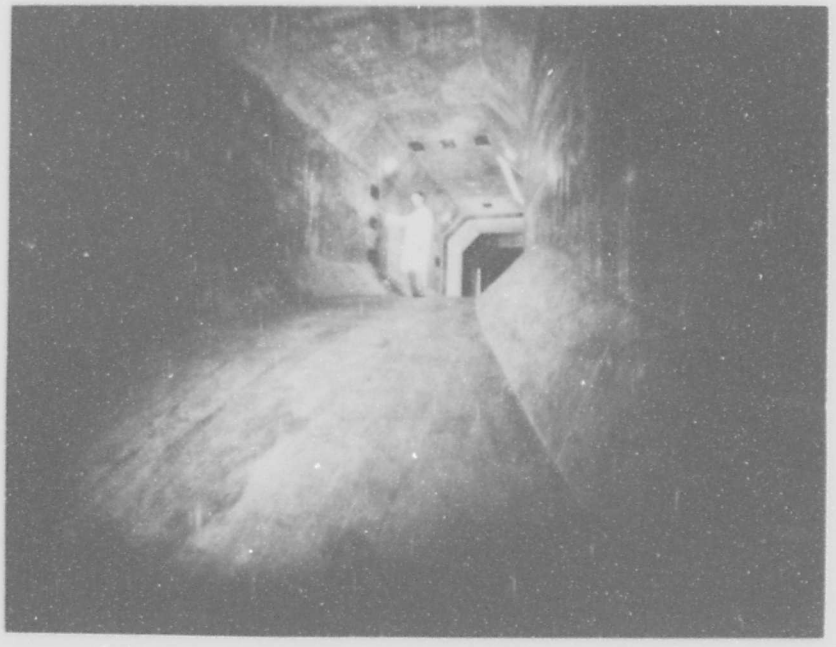

Figure 9 - Photograph of Concrete Contraction Section (10:1 Contraction Ratio)

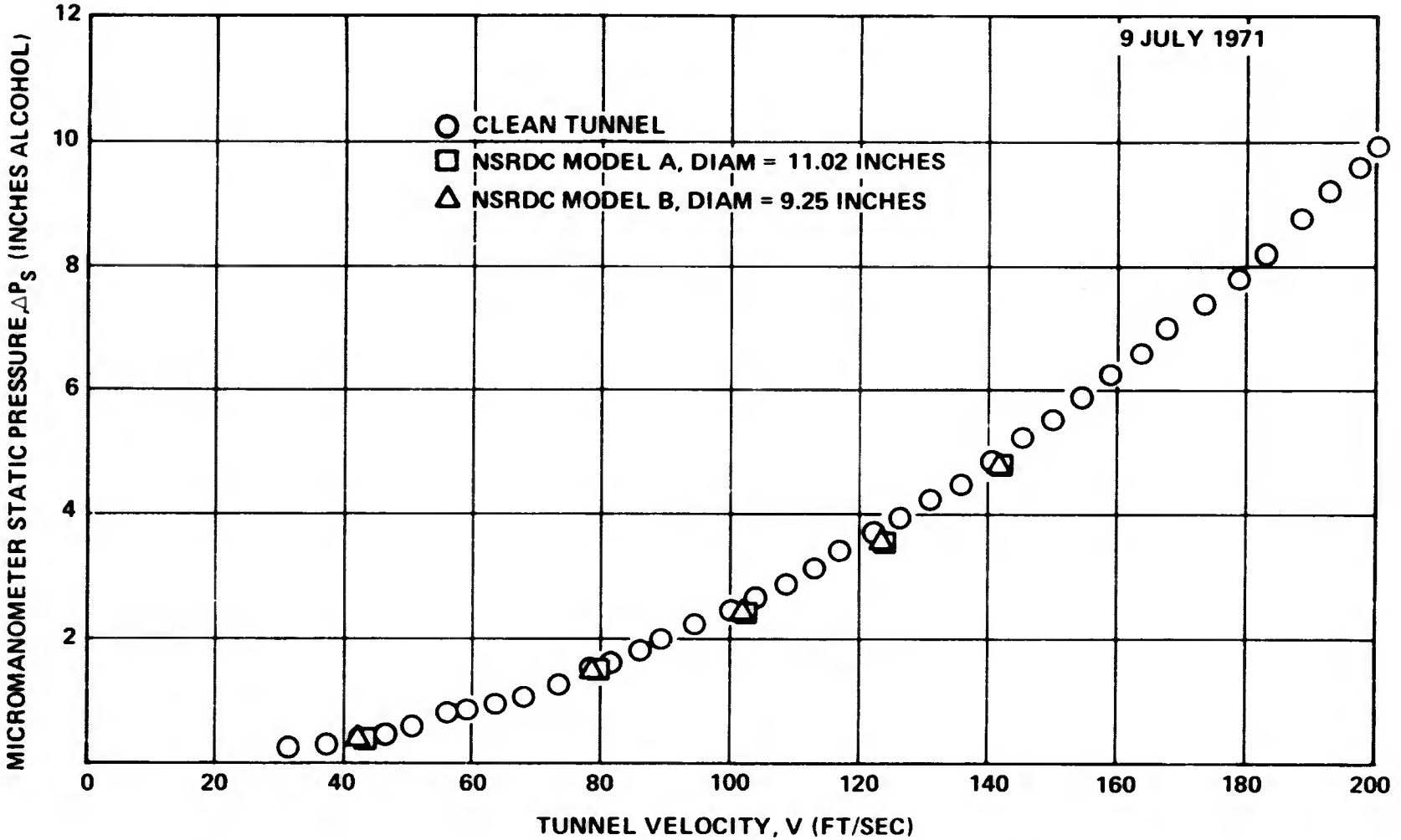

Figure 10 - Clean Tunnel Velocity Calibration and Solid Blockage Interference Effect for Two Typical Bodies-of-Revolution

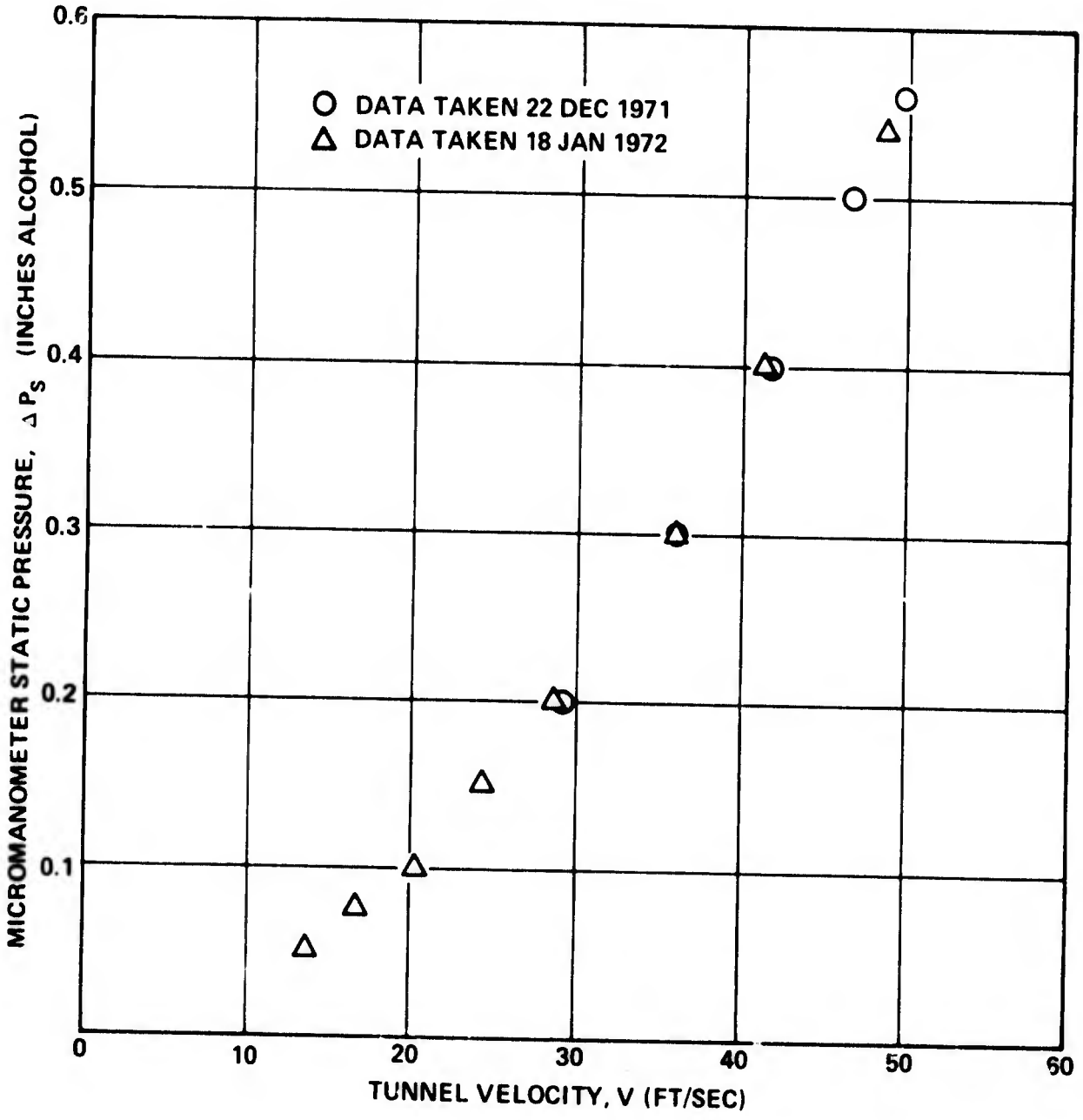

Figure 11 - Low Speed Tunnel Velocity Calibration

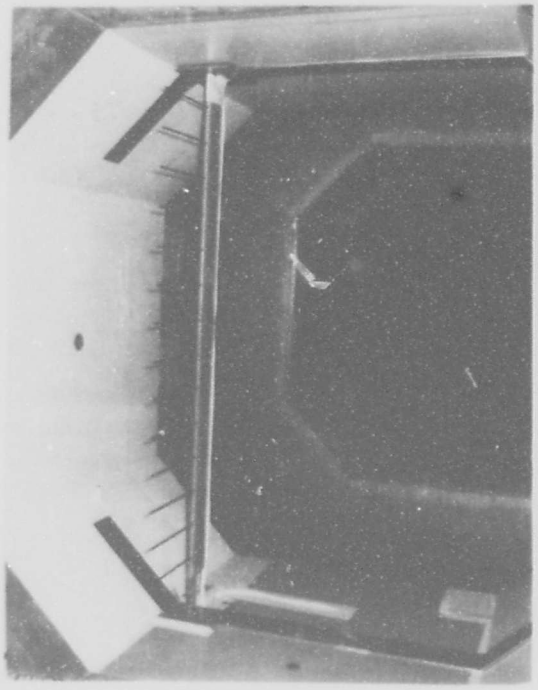

Figure 12 - Vertical Mounting of Survey Rake to Determine Cross-Sectional Velocity Profile

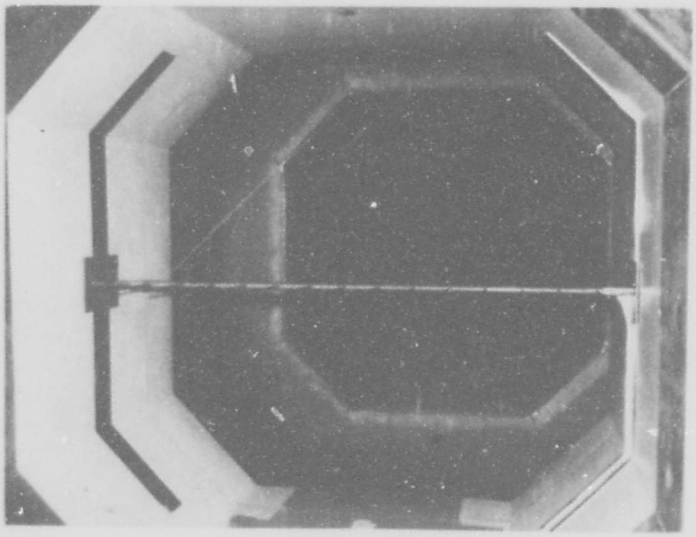

Figure 13 - Horizontal Mounting of Survey Rake to Determine Cross-Sectional Velocity Profile

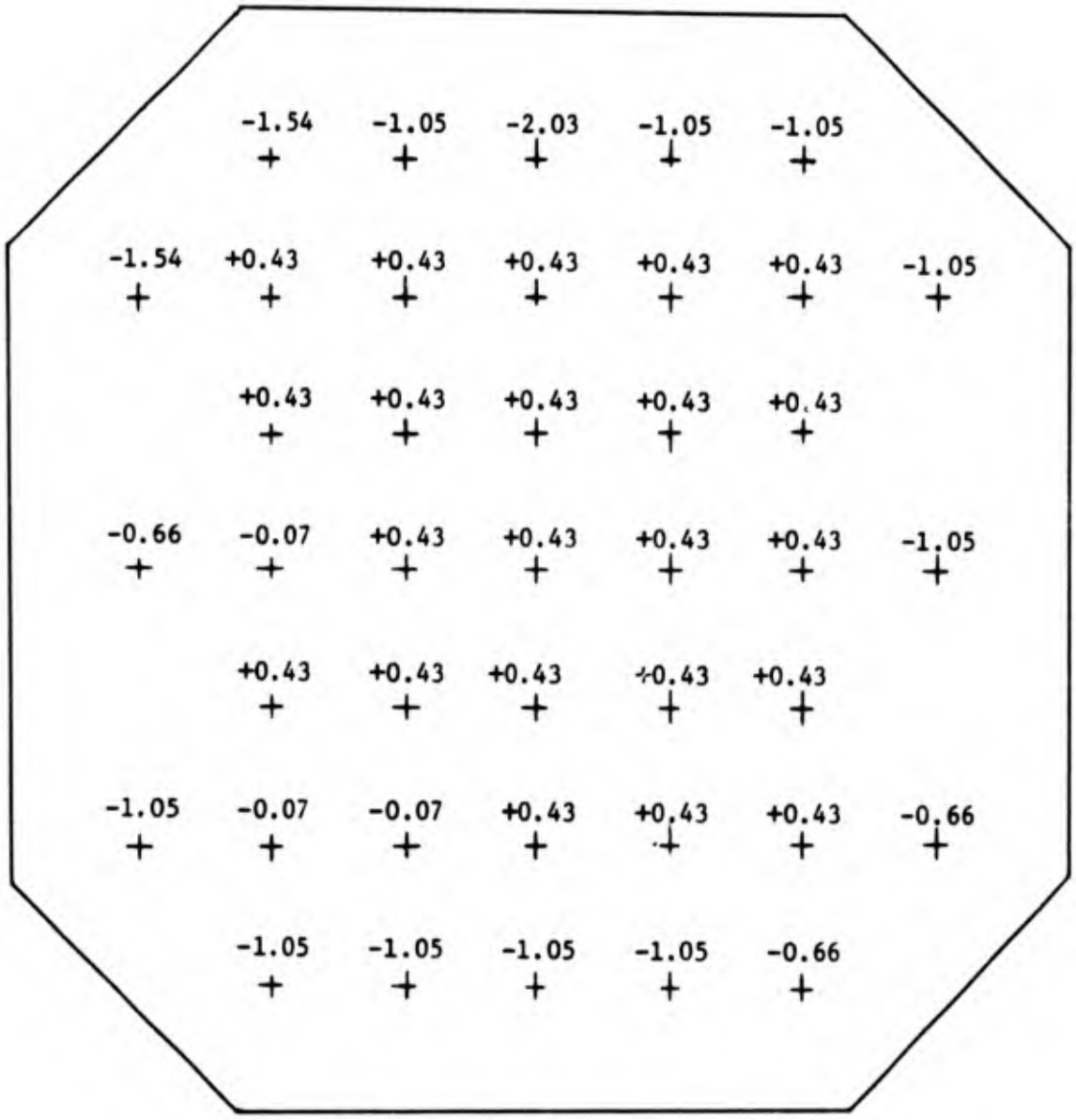

Figure 14 - Typical Cross-Sectional Velocity Distribution in the Closed-Jet Test Section, 53 3/16 inches from Nozzle Lip. Values shown are the Percentage Deviations from the Mean Velocity of 203.1 fps. Experimental Error is $\pm$ 0.5%.

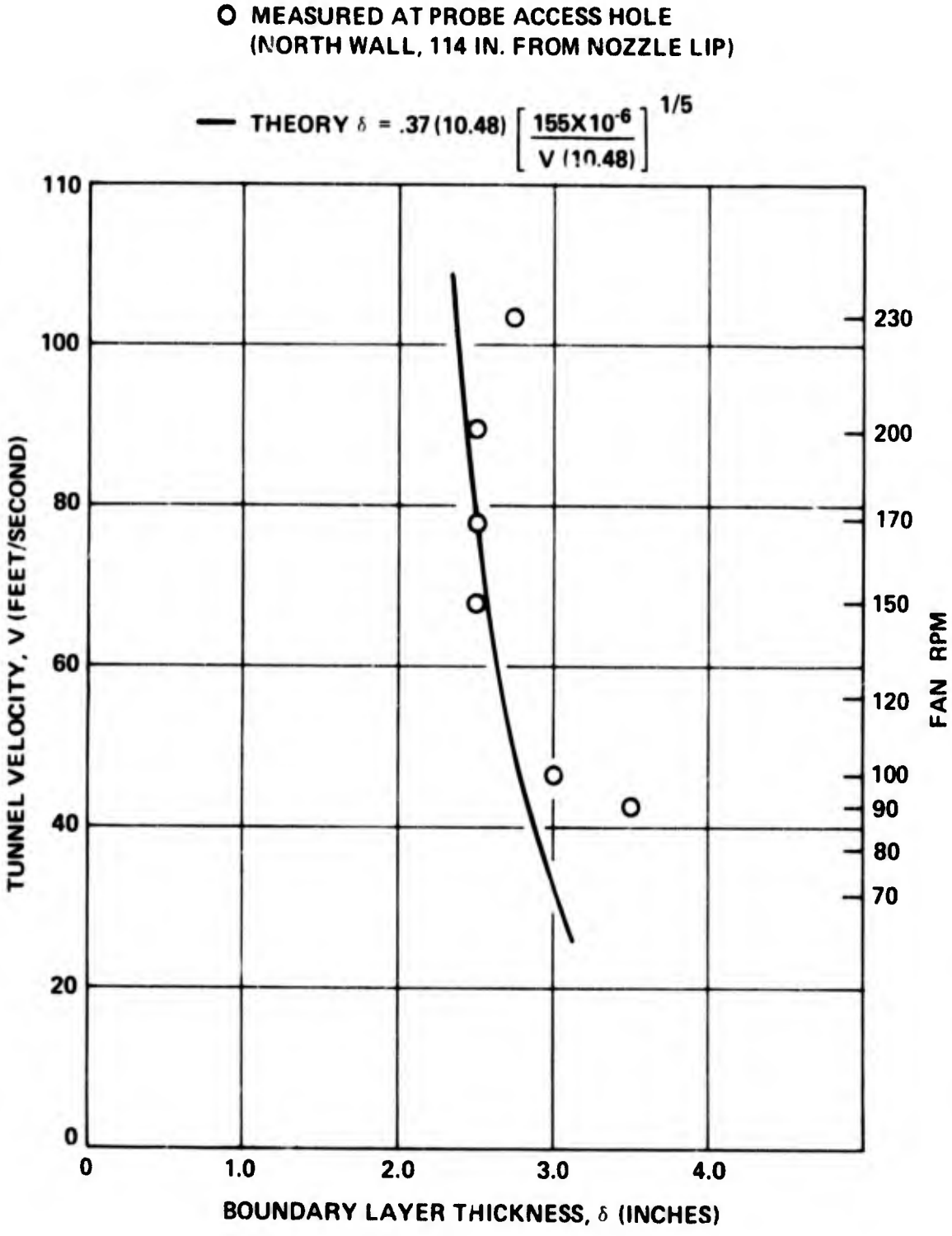

Figure 15 - Boundary Layer Thickness Measurements at Probe Access Hole Compared to Theoretical Prediction (Ref. 5) Using Virtual Leading Edge at X = 10.48 Ft.

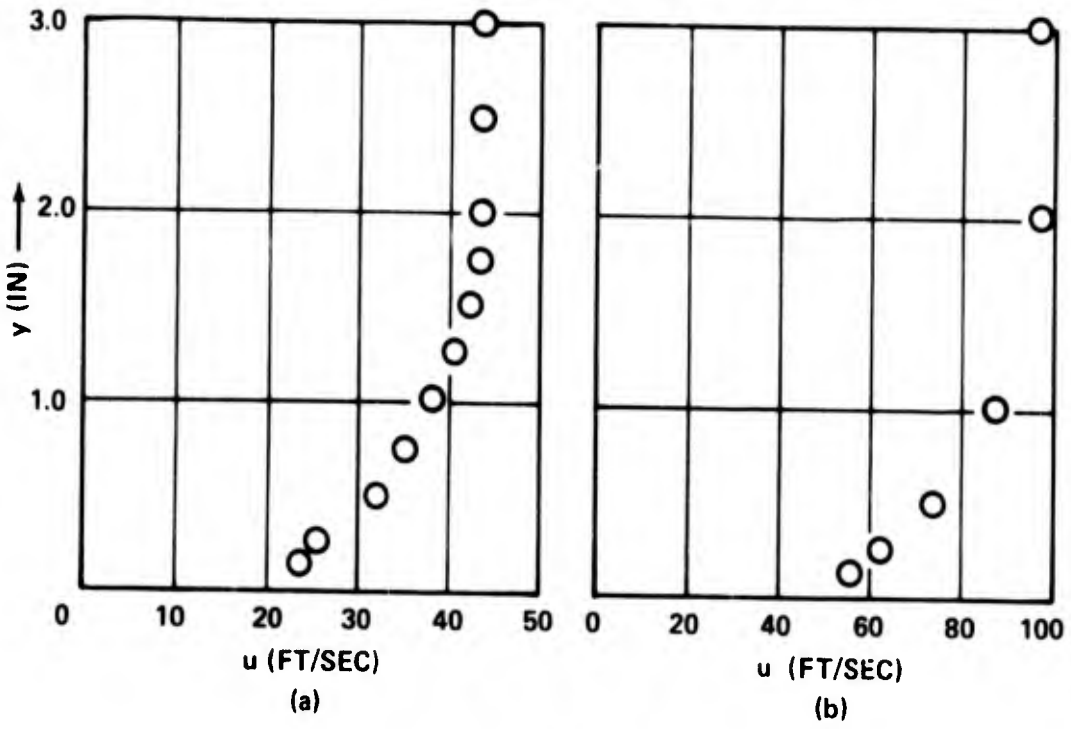

Figure 16 - Boundary Layer Velocity Gradient on Floor, 5.375 In. from Flat Plate and 187.75 In. from Nozzel Lip

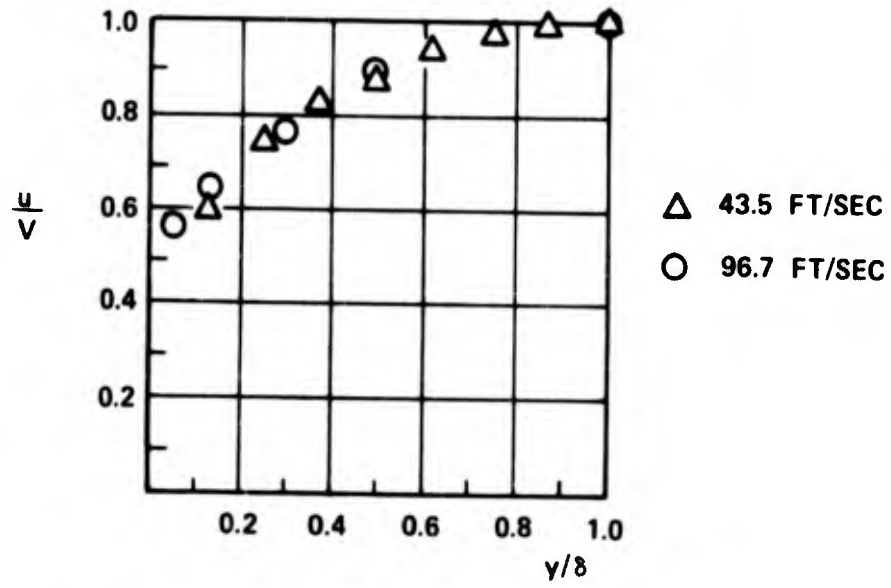

Figure 17 - Boundary Layer Profiles on Floor

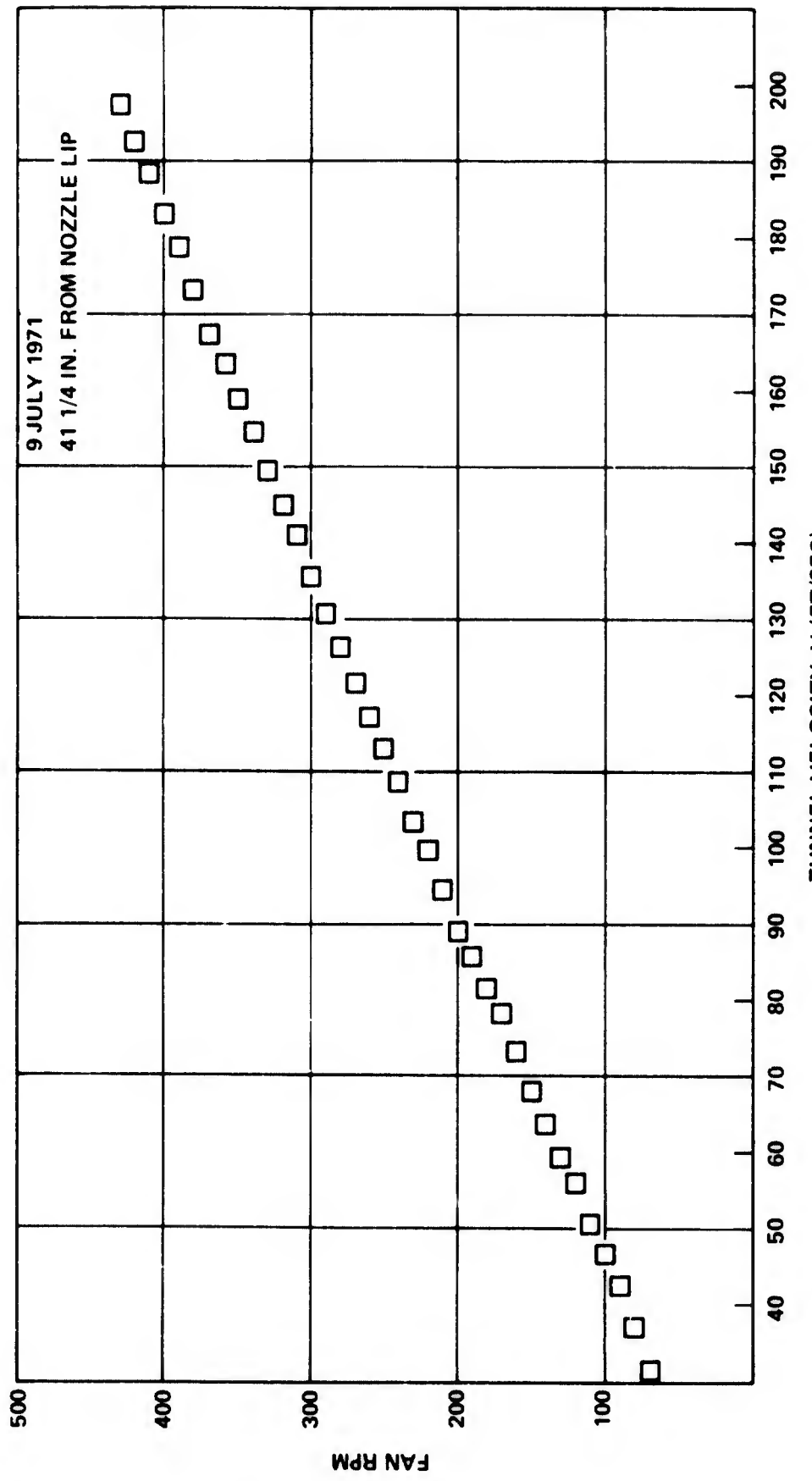

Figure 18 - Variation of Tunnel Velocity with Fan RPM

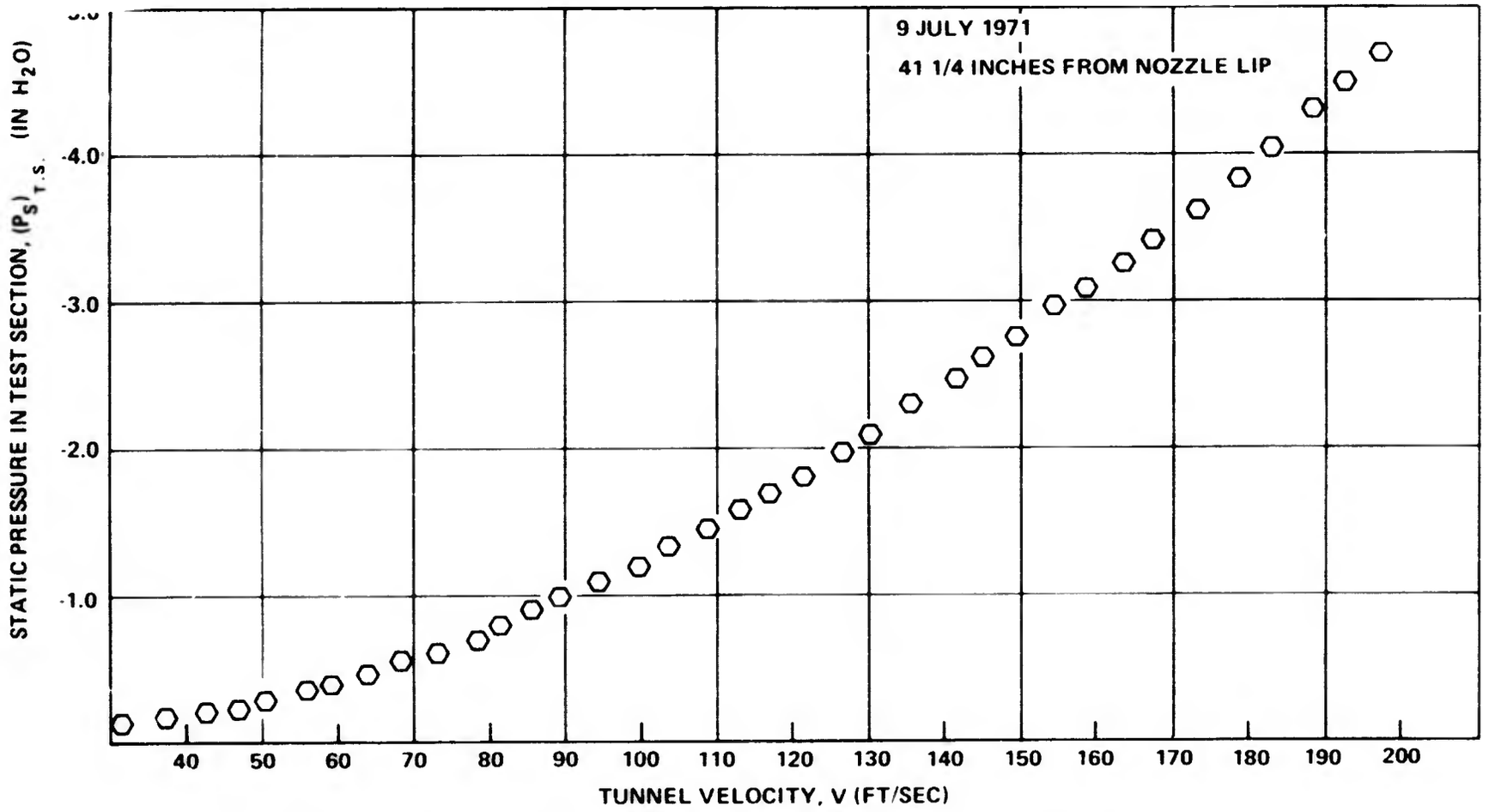

Figure 19 - Variation of Test Section Static Pressure with Tunnel Velocity

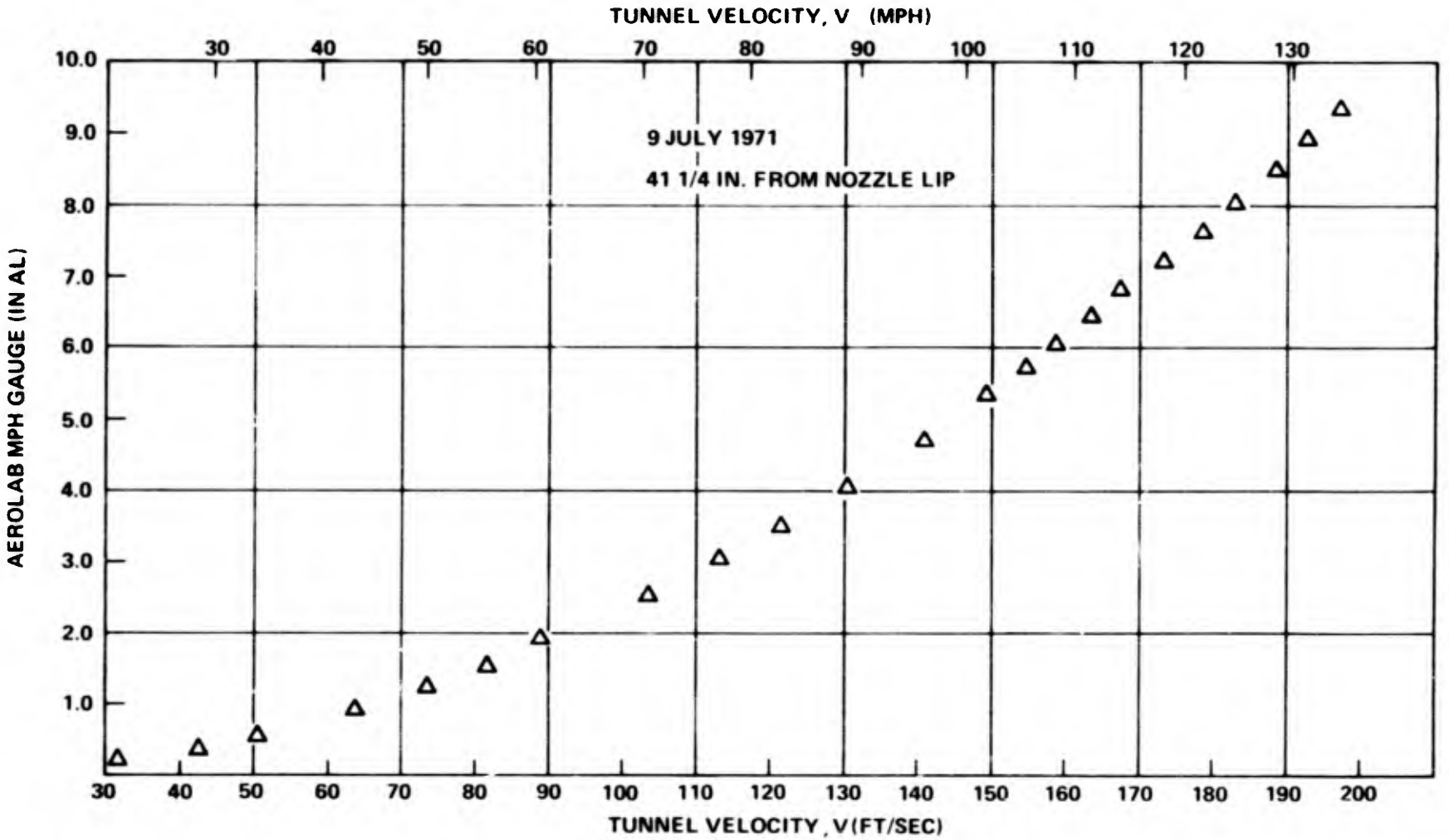

Figure 20 - Calibration of Wall Mounted MPH Gauge

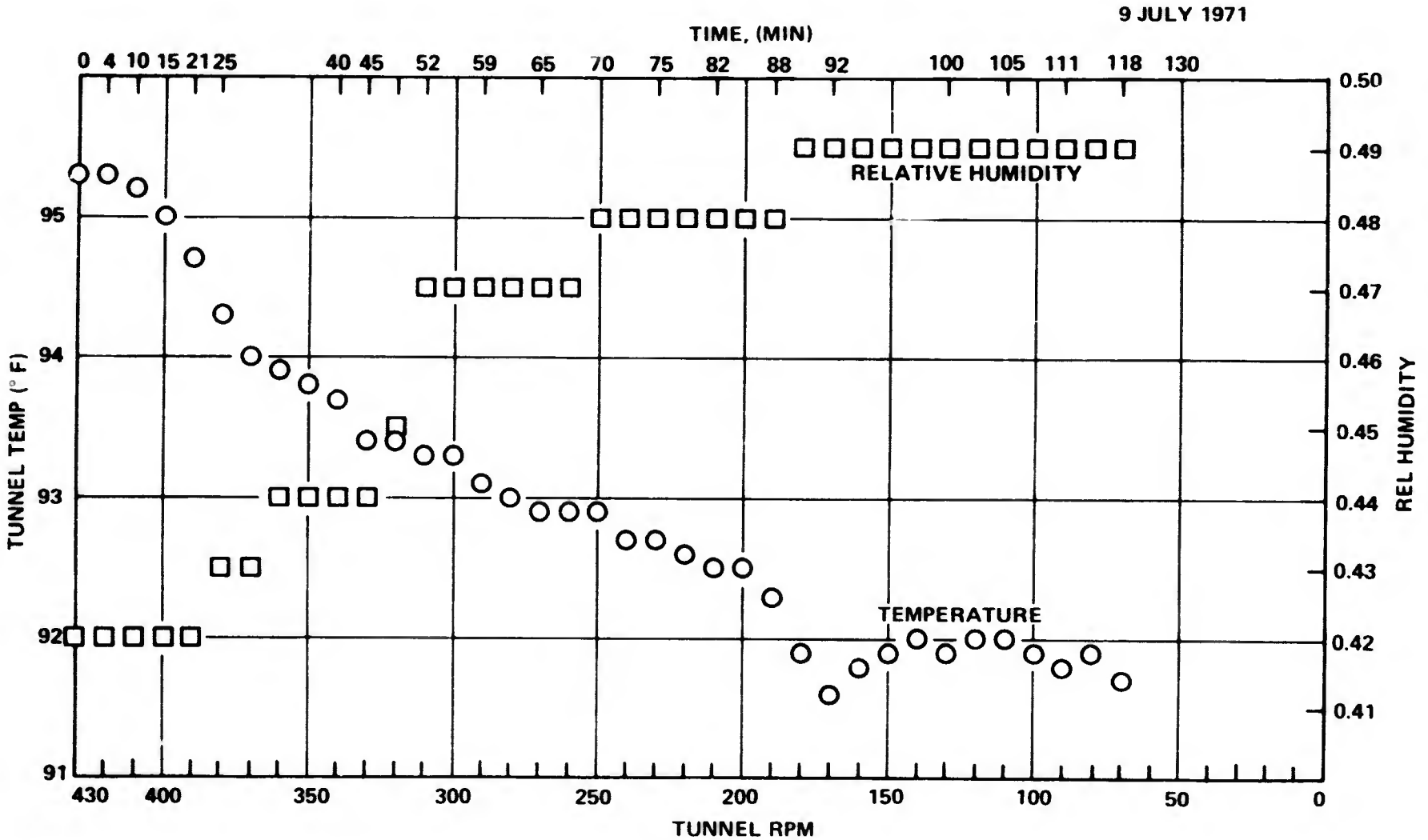

Figure 21 - Typical Tunnel Temperature and Humidity Variation with Fan RPM
(Tunnel Cooling Off)

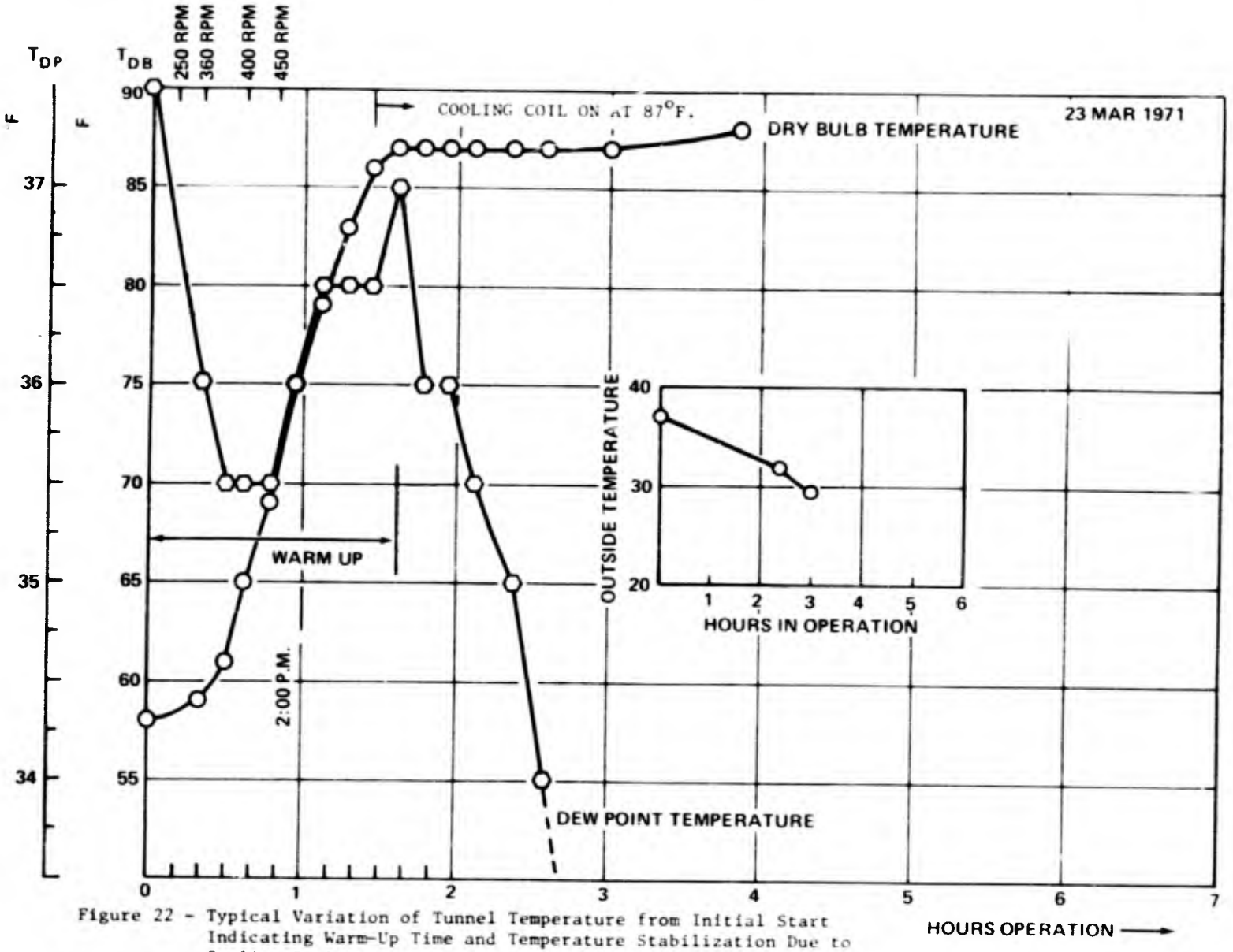

Figure 22 - Typical Variation of Tunnel Temperature from Initial Start Indicating Warm-Up Time and Temperature Stabilization Due to Cooling Coil

TABLE 1

SUMMARY OF HOT WIRE TURBULENCE INTENSITY MEASUREMENTS CARRIED OUT IN CLOSED-JET TEST SECTION

Investigator	Anemometer Used	Location of Probe, in.	Tunnel Condition	Measured Turbulence Intensity, %	Tunnel Velocity, ft/sec
Bowers Mathews DeMetz	Flow Corp. model 900F const. temp.	Longitudinal centerline, 43.25 from nozzle lip, mounted on sting	Clean	0.14	200
Dwyer Blake	Disa model 55 D05 const. temp. battery powered	Longitudinal centerline, 24 from nozzle lip, mounted on mic, pos. sys	Clean	0.122 0.115	100 200
DeMetz Stern	Flow Corp. model 900F const. temp.	2 from plate, 46 from south wall, 144 from nozzle lip, mounted on flat plate pos. device	Flat Plate Prototyp Model	0.086 0.076 0.060 0.065	50.5 148.1 50.7 148.9
DeMetz Stern Helmandollar	Flow Corp. model HWB-3 const. current battery powered	12.75 from north wall wall, 127.75 from nozzle lip	10 ft. model submarine (downstream of probe)	0.092 0.076 0.068	50 100 120
DeMetz Helmandollar	Flow Corp. model HWB-3 const. current battery powered	Longitudinal centerline, 72 from nozzle lip, mounted on sting	Clean	0.123 0.130 0.095 0.092	100 100 200 200
DeMetz Helmandollar	Flow Corp. Model HWB-3 constant current battery powered	Line defined by horiz. centerplane and vertical plane located at 45.125 from nozzle lip	Clean	(Probe location and measurements on next page)	

TABLE 1 (Cont.)

Investigator	Anemometer Used	Location of Probe, in.	Tunnel Condition	Measured Turbulence Intensity, %	Tunnel Velocity, ft/sec
		11.875 from south wall		0.135	100
				0.131	200
		23.813 from south wall		0.167	100
				0.117	200
		35.938 from south wall		0.116	100
				0.087	200
		48.000 from south wall		0.124	100
				0.094	200
		83.938 from south wall		0.115	100
				0.095	200

REFERENCES

1. Brownell, W.F., "An Anechoic Flow Facility Design for the Naval Ship Research and Development Center, Carderock," NSRDC Report 2924, (Sep 1968)

2. Schubauer, G.B. and Spangenberg, W.G., "Effect of Screens in Wide Angle Diffusers," NACA Report 949, (1949)

3. Northern Research and Engineering Corporation, "Model Studies of the DTMB Anechoic Test Facility," Report No. 1074-1 (14 Feb 1964)

4. Jorgensen, R., Editor, "Fan Engineering," Sixth Edition, Buffalo Forge Co., Buffalo, N.Y. (1961)

5. Schlichting, H., Boundary-Layer Theory, 6th Edition, McGraw-Hill (1968)